ACS OMEGA

http://pubs.acs.org/journal/acsodf

Article

Fabrication and Characterization of Cu Nanoparticles Dispersed on ZnAl-Layered Double Hydroxide Nanocatalysts for the Oxidation of Cyclohexane

Jagat Singh Kirar,* Neeraj Mohan Gupta, Kailash Chandra, Hitesh Kumar Vani, Savita Khare, Neha Tiwari, and Yogesh Deswal

Cite This: *ACS Omega* 2022, 7, 41058−41068

Read Online

ACCESS | Metrics & More | Article Recommendations

ABSTRACT: In the chemical industry, designing high-performance catalysts for the oxidation of cyclohexane into value-added products such as cyclohexanol and cyclohexanone (the combination is known as KA oil) is critical. The catalytic activity of copper nanoparticles supported on layered double hydroxide (LDH) for the liquid phase oxidation of cyclohexane was examined in this study. In this work, we have developed Cu nanoparticles supported on layered double hydroxide nanocatalysts, abbreviated as CuNPs@LDH, by the chemical reduction approach. Various physical methods were used to characterize the resulting material, including ICP-AES, XRD, FTIR, SEM, EDX, HRTEM, and BET surface area. The catalytic activity of copper nanoparticles supported on LDH was examined for the liquid phase oxidation of cyclohexane with *tert*-butyl hydroperoxide. CuNPs@LDH nanocatalysts with an excellent 52.3% conversion of cyclohexane with 97.2% selectivity of KA oil was obtained after 6 h at 353 K. The hot filtration test further indicated that CuNPs@LDH was a heterogeneous catalyst that could be recycled at least six times without suffering a substantial reduction in its catalytic activity.

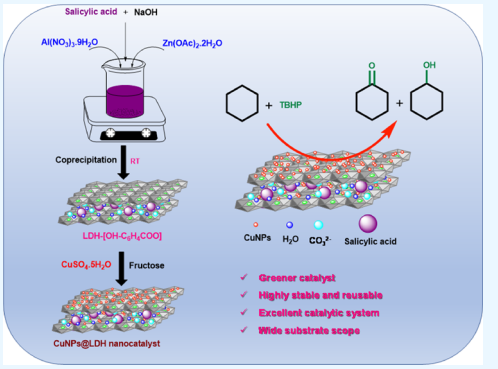

1. INTRODUCTION

The development of catalysts for the selective oxidation of cyclohexane under moderate conditions with environmentally benign oxidants is of academic as well as industrial interest.[1,2] Catalytic oxidation of cyclohexane is one of the most challenging reactions due to the high stability of the C−H bond.[3,4] The oxidation products cyclohexanol and cyclohexanone are known as KA oil, which is the important raw material of adipic acid and caprolactam used as a precursor in the manufacturing of nylon-6 and nylon-66 polymers.[5,6] Generally, to obtain higher selectivity (70−80%) in the oxidation of cyclohexane, certain procedures using soluble Co and Mn salts are frequently used as catalysts and the conversion efficiency was found to be quite low (5%).[5,7] As a result, high-efficiency heterogeneous catalysts for selective oxidation of cyclohexane are desirable. Heterogeneous catalysts have evident benefits in terms of easier catalyst separation from the reactant, recycling, and better at meeting the demands of sustainable chemistry.[2,8,9] Therefore, several researchers have worked hard to design a suitable heterogeneous catalytic system for the oxidation of cyclohexane. Several catalytic systems have lately been investigated, with transition metal catalysts getting the most attention.[10−19] Han et al. described the fabrication of transition metal oxide/graphene composites as heterogeneous catalysts for cyclohexane oxidation. Under optimal conditions, a maximum of 34.4% conversion of cyclohexane with 74.4% selectivity of KA oil was achieved after 6 h over the CoO/graphene catalyst.[10] Liu et al. developed hydrotalcite-derived Co-MgAlO-mixed metal oxides as stable and efficient heterogeneous catalysts for the selective aerobic oxidation of cyclohexane to KA oil. The catalyst Co-MgAlO is active and selective for the oxidation of cyclohexane. The synergistic catalysis of Co^{3+} and Co^{2+} may efficiently enhance the decomposition of the cyclohexyl hydroperoxide (CHHP) intermediate to KA oil. A maximum of 9.1% of cyclohexane conversion and 82.0% of KA oil selectivity over 2% Co-MgAlO catalysts were obtained at 423 K and 0.6 MPa for 2 h in this oxidation reaction.[11] Jian et al. synthesized a Cu-MgAlO catalyst derived from hydrotalcite for the partial oxidation of cyclohexane with molecular oxygen. According to the findings, copper, as the active species, could activate the C−H bond and successfully enhance the decomposition of CHHP to KA oil. A maximum of 8.3% of cyclohexane conversion and 82.9% of

Received: July 13, 2022
Accepted: October 13, 2022
Published: November 1, 2022

https://doi.org/10.1021/acsomega.2c04425
ACS Omega 2022, 7, 41058−41068

Scheme 1. Schematic Representation of the Synthesis of LDH−[OH−C_6H_4COO] and CuNPs@LDH

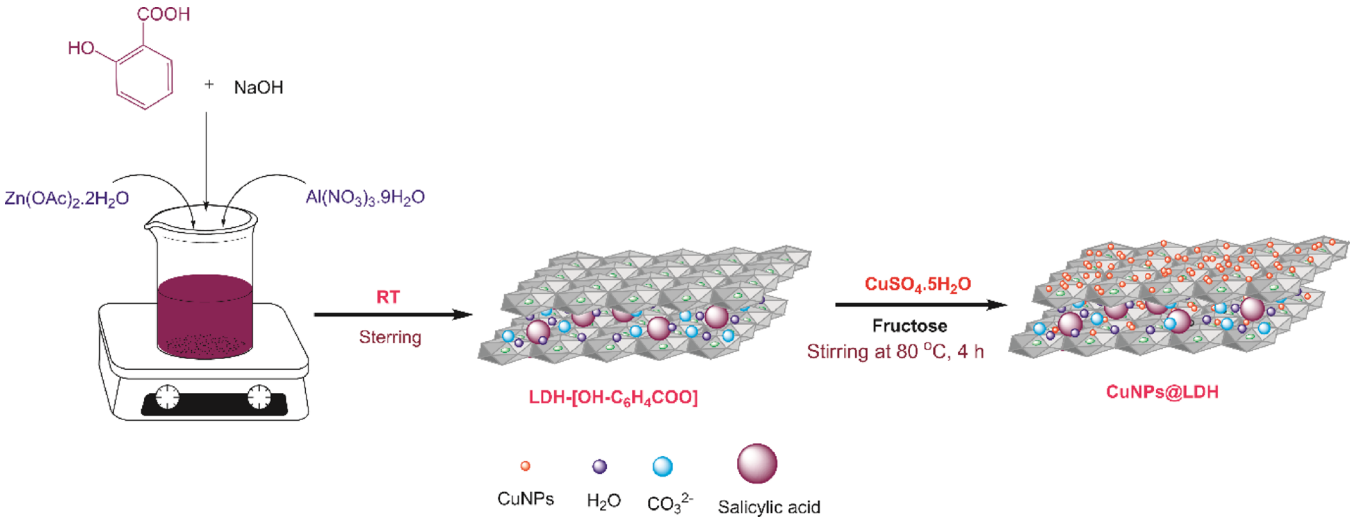

Table 1. Analytical Data and Textural Properties of LDH−[OH−C_6H_4COO] and the CuNPs@LDH Nanocatalyst

				elemental composition (wt%)				
catalysts	metal contents[b] (%)	*d*-spacing (Å)	BET surface area (m^2/g)	Zn	Al	C	O	Cu
LDH	-	15.43	18.26	37.82	7.0	15.58	39.61	-
CuNPs@LDH	5.41	15.38	49.85	44.34	5.96	8.94	30.83	9.94
CuNPs@LDH[a]	5.33	15.27	-	43.61	5.48	9.53	31.88	9.50

[a]Reused nanocatalyst. [b]ICP-AES.

selectivity for KA oil were achieved over 9%Cu-MgAlO catalysts at 150 °C with 0.6 MPa of oxygen pressure for 2 h.[12] Ziouèche et al. reported catalytic activity of MCoS(20) for the oxidation of cyclohexane with *tert*-butyl hydroperoxide and obtained 22.3% cyclohexane conversion with 95.3% KA oil selectivity. The results show that when water-free TBHP is employed, the catalysts become more active.[13]

Particle size plays a key role in catalytic reactions because the catalytic reaction takes place on the metal surface of the catalyst, and it is reasonable to assume that smaller metal particles have more surface area and hence more activity. The immobilization of nanoparticles on the surface of insoluble inorganic supports has attracted a lot of interest.[20−24] However, to the best of our knowledge, the investigation of Cu nanoparticles supported on layered double hydroxide as a nanocatalyst for the oxidation of cyclohexane is rarely reported.

On the other hand, layered double hydroxides (LDHs) have the general formula $[M^{II}_{1-x}M^{III}_{x}(OH)_2]^{x+}.(A^{n-}_{x/n}).mH_2O$ and attract a great deal of attention as an ideal catalyst support due to their attractive properties such as expansion capabilities, anion exchange properties, large surface area, chemical inertness, high ion exchange, nature of interlayer anions, and tunable basicity.[25,26] LDHs have become the material of choice for the manufacture of heterogeneous catalysts with relevant physical and chemical characteristics due to their unique adjustable features. Because of the presence of basic hydroxyl groups, LDHs have been widely employed as heterogeneous catalysts for base-catalyzed processes.[27] The high adsorption capacity of LDH makes it an ideal support for immobilizing catalytically active species.[28] Furthermore, uniform dispersion of M(II) and M(III) cations in the LDH layers, as well as anion-preferred orientations in the interlayer, is a useful feature for using LDH as precursors for the fabrication of stably supported catalysts. We have recently synthesized transition metal Schiff base complexes based on LDHs as heterogeneous catalysts and tested their catalytic activity for oxidation of toluene.[29,30]

In this paper, we have adopted a simple chemical reduction approach to synthesize CuNPs@LDH that may function as a heterogeneous nanocatalyst for the selective oxidation of cyclohexane using *tert*-butyl hydroxide as an oxidant. To improve the reaction conditions for obtaining optimum conversion of cyclohexane and selectivity of KA oil, we have studied various parameters such as the influence of different oxidants, influence of the TBHP to cyclohexane molar ratio, influence of the catalyst amount, influence of temperature, and influence of time. A hot filter experiment was also employed to investigate metal leaching, as well as possible mechanisms.

2. RESULTS AND DISCUSSION

2.1. Characterization of Nanocatalysts. The Cu nanoparticles supported on LDH, CuNPs@LDH nanocatalysts are synthesized using the procedure described in Scheme 1. Table 1 shows the analytical and physical data of compounds, including chemical composition, at various stages of the synthesis of LDH−[OH−C_6H_4COO], CuNPs@LDH, and reused CuNPs@LDH. Fresh CuNPs@LDH contains 5.41% copper contents, whereas CuNPs@LDH[a] contains 5.33% copper after six catalytic cycles, as measured by ICP-AES. The ICP-AES data indicate that metal leaching did not occur throughout the cyclohexane oxidation reaction.

Figure 1 shows the X-ray diffraction (XRD) patterns of LDH−[OH−C_6H_4COO], CuNPs@LDH, and reused CuNPs@LDH nanocatalysts. The most intense basal reflection is seen in the XRD pattern of LDH−[OH−C_6H_4COO] at 15.43 (003). The typical reflections in the (110) plane illustrate the atomic distribution density as a function of the Zn:Al molar

https://doi.org/10.1021/acsomega.2c04425
ACS Omega 2022, 7, 41058−41068

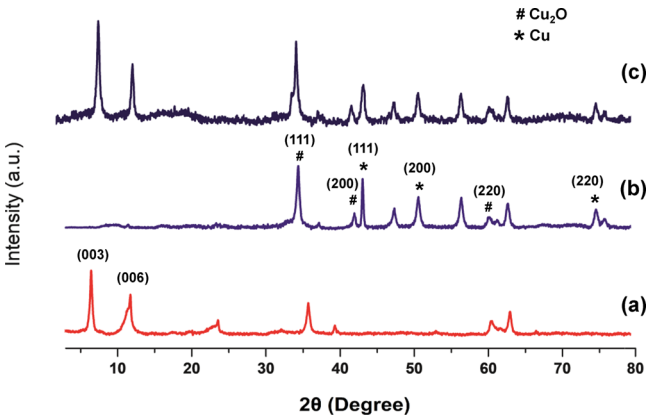

Figure 1. XRD pattern of (a) LDH−[OH−C_6H_4COO], (b) CuNPs, and (c) CuNPs@LDH.

ratio. The existence of two strong and narrow diffraction lines corresponding to (003) and (006) reflections of a crystalline ZnAl-LDH phase is shown by the XRD patterns of LDH−[OH−C_6H_4COO].[31−33] The occurrence of (003) and (006) illustrates the formation of the lamellar structure of LDH, intercalated with water and salicylic acid ions.[34] There are no other peaks that may be attributed to other phases or impurities, indicating that the ZnAl-LDH phase is pure. Furthermore, the XRD patterns of CuNPs@LDH show two crystalline phases, metallic Cu and Cu_2O. This clearly shows that the zero-valent Cu nanoparticles produced during the chemical reduction step go through decomposition due to the limited stability of Cu, and Cu_2O may be formed by oxidation.[35] The XRD reflections at 42.4°, 50.5°, and 74.53° correspond to metallic Cu crystal faces (111), (200), and (220), respectively, and the Cu_2O phase at 36.43°, 42.21°, and 61.11° is indexed as (111), (200), and (220), respectively.[36,37] Cu nanoparticles have been effectively adsorbed on ZnAl-LDH support, according to XRD, EDX, and ICP-AES results, which verified the presence of copper.

The scanning electron microscopy (SEM) analysis was used to examine the surface morphology of ZnAl-LDH and CuNPs@LDH. The results are depicted in Figure 2a−d. The SEM images

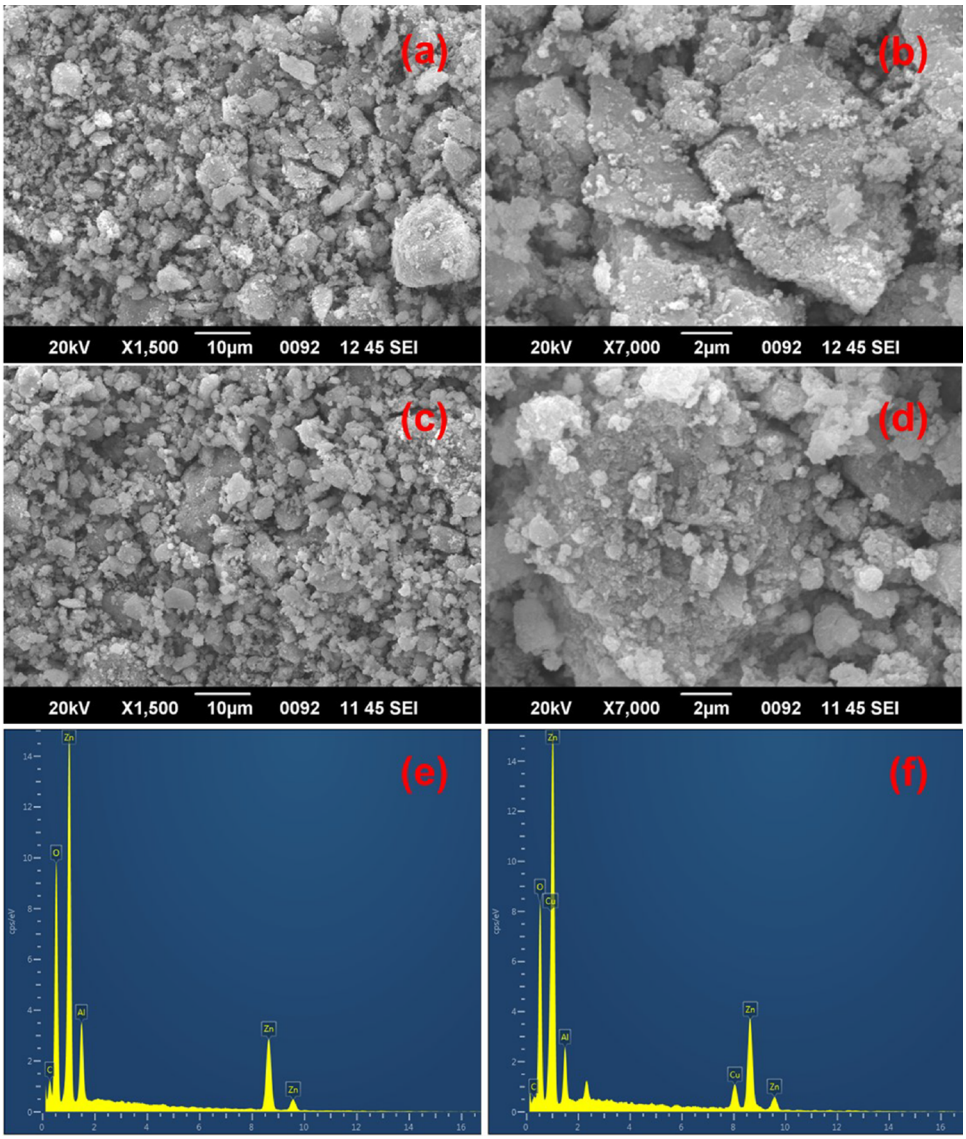

Figure 2. SEM images of (a,b) LDH−[OH−C_6H_4COO] and (c,d) CuNPs@LDH. EDX spectra of (e) LDH−[OH−C_6H_4COO] and (f) CuNPs@LDH.

https://doi.org/10.1021/acsomega.2c04425
ACS Omega 2022, 7, 41058−41068

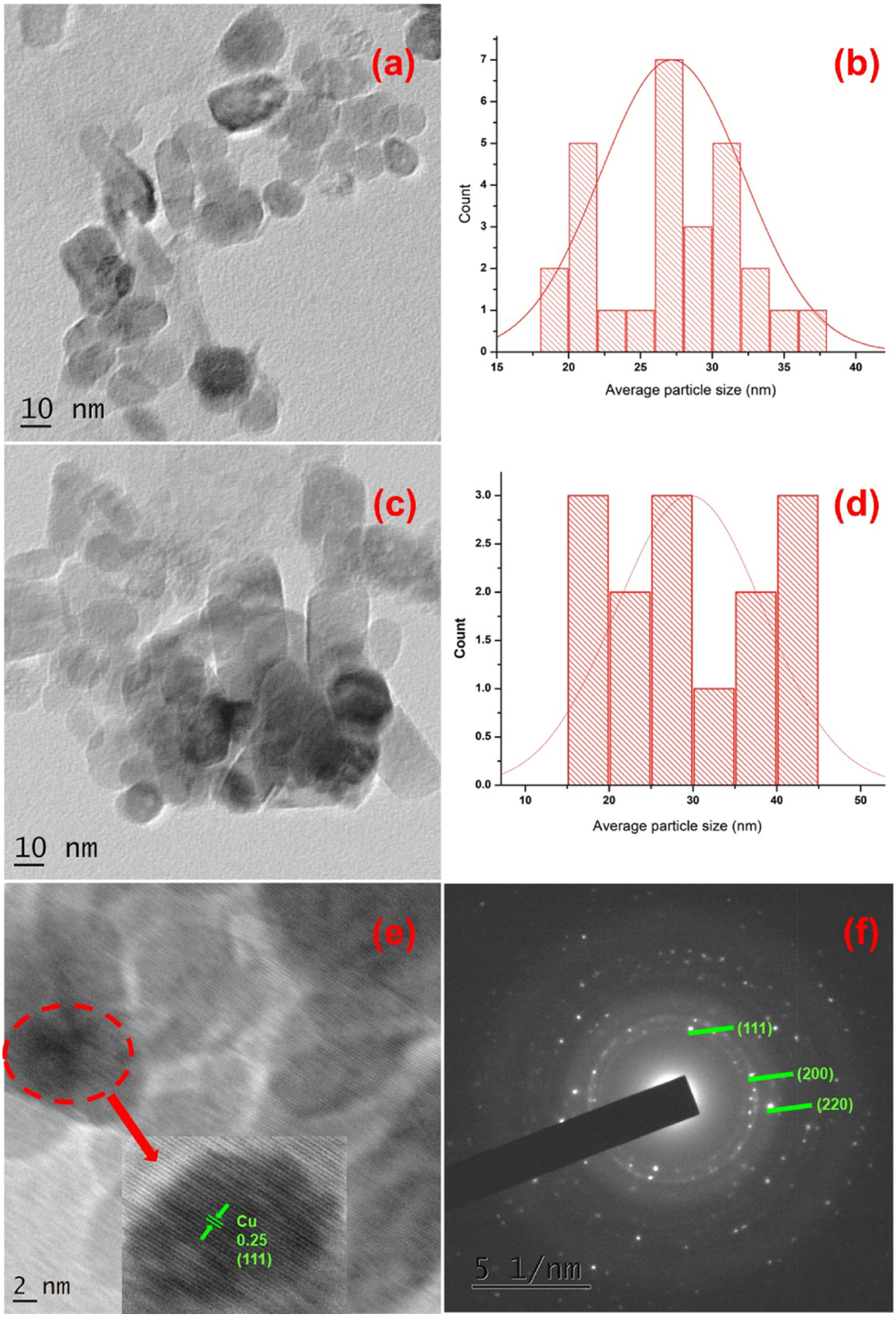

Figure 3. HRTEM images and particle size distribution of (a,b) LDH−[OH−C_6H_4COO] and (c,d) CuNPs@LDH. HRTEM images at high magnification of (e) CuNPs@LDH; SAED images of (f) CuNPs@LDH.

revealed a distinct lamellar and nanoplatelet structure, confirming that the layered double hydroxide initial lamellar organization was intact in the CuNPs@LDH nanocatalyst. The surface also had some imperfections, indicating that it had a high adsorption capacity. The SEM images also showed that the crystallinity of the nanocatalyst corresponded to the XRD

https://doi.org/10.1021/acsomega.2c04425
ACS Omega 2022, 7, 41058−41068

pattern's characteristic reflections.[24] Figure 2e,f shows the chemical composition of the nanocatalyst as determined by EDX analysis. The nanocatalyst, CuNPs@LDH, contains carbon, oxygen, zinc, aluminum, and copper metals, indicating that a heterogeneous nanocatalyst has successfully synthesized.

The samples have a thin plate-shaped crystalline morphology with layered structures, as shown in the HRTEM images in Figure 3. The shapes of the brucitelike layers were retained after reduction. Figure 3b,d depicts the average particle size distribution of LDH−[OH−C_6H_4COO] and CuNPs@LDH, with particle size ranging from 20 to 50 nm.[38] The HRTEM study of CuNPs@LDH revealed that Cu nanoparticles are uniformly dispersed over the LDH platelets (Figure 3c,e).[39] Furthermore, HRTEM images shown in Figure 3e revealed an interplanar spacing of 0.25 nm, which is consistent with the interplanar distance of the Cu (111) crystallographic plane, which is consistent with the powder XRD results (Figure 1b).[38,40] Additionally, no diffraction patterns of Cu^+ species were found, which was consistent with the XRD results. Cu nanoparticles were highly dispersed and tightly anchored on the LDH due to the layered structures in CuNPs@LDH. The HRTEM image of CuNPs@LDH (Figure 3c) shows a lot of Cu dark spots dispersed in LDH−[OH−C_6H_4COO] sheets. These findings strongly suggest that the Cu particles were distributed uniformly on the LDH−[OH−C_6H_4COO] frameworks and that the reduction process did not affect the structure of LDH−[OH−C_6H_4COO].

The selected area electron diffraction (SAED) pattern of CuNPs@LDH is shown in Figure 3f. A typical *d*-spacing of 0.25 nm for (111) is shown in Figure 3f. The planes (200) and (220) are indexed in the SAED pattern of polycrystalline diffraction rings, demonstrating the single-crystalline nature of the Cu nanoparticles. It demonstrates that CuNPs@LDH particle size ranges from 20 to 50 nm.

The catalytic activity of the catalyst depends on the surface area of the catalyst. Therefore, the surface area of the catalyst plays a key role in catalytic reactions. The surface areas of LDH[OH−C_6H_4COO] and CuNPs@LDH were measured by BET surface area analysis. The results are incorporated in Table 1. The surface area of LDH−[OH−C_6H_4COO] was determined to be 18.26 m^2/g, whereas CuNPs@LDH had a surface area of 49.85 m^2/g. CuNPs@LDH has a larger surface area, which helps to maintain the dispersion of copper nanoparticles and improves their catalytic efficiency.

Figure 4 shows the Fourier transform infrared (FTIR) spectra of LDH−[OH−C_6H_4COO] and CuNPs@LDH. The broad absorption bands at 3395 cm^{-1} in the LDH−[OH−C_6H_4COO] spectrum (Figure 4a) were attributed to the hydroxyl group, OH stretching mode. The C═O stretching vibration of the carboxylic group of salicylic acid is responsible for the strong band at 1737 cm^{-1}. The bands at 1456 and 1387 cm^{-1} can be attributed to aromatic ring C═C stretching and NO_3^- ions, respectively.[41] Stretching vibrations of M−O and O−M−O (M = Zn and Al) cause the bands in the range of 455−761 cm^{-1}, which is typical of this class of materials.[42] Most of the chemical layered structure of LDH appears to be unaffected after Cu incorporation in LDH, based on these findings.

2.2. Catalytic Activity Studies. Our major objective was to design a simple, efficient, and environmentally acceptable approach for oxidation reaction using CuNPs@LDH, given the importance of functionalized carbonyl compounds. To optimize the reaction conditions, we have explored the oxidation of cyclohexane in a solvent-free environment using TBHP as an oxidant. Under optimum reaction conditions, the catalytic activity of LDH and CuNPs@LDH for the oxidation of cyclohexane was investigated, as well as that in a blank reaction. Table 2 summarizes the findings. Cu nanoparticles exhibit up to 34.6% low cyclohexane conversion with 95.1% KA oil selectivity, whereas the CuNPs@LDH nanocatalyst exhibits 52.3% cyclohexane conversion with 97.2% KA oil selectivity and other products (cyclohexyl hydroperoxide, adipic acid, glutaric acid, succinic acid, hydroxyl hexylic acid, and ε-caprolactone).[43] The CuNPs@LDH nanocatalyst has basic sites provided by ZnAl-LDH and a large surface area compared to Cu nanoparticles. It was observed that the support, ZnAl-LDH, was inactive for the oxidation of cyclohexane. When the reaction was carried out in the absence of either a nanocatalyst or an oxidant, no products were produced in blank reactions. Thus, auto-oxidation was ruled out.

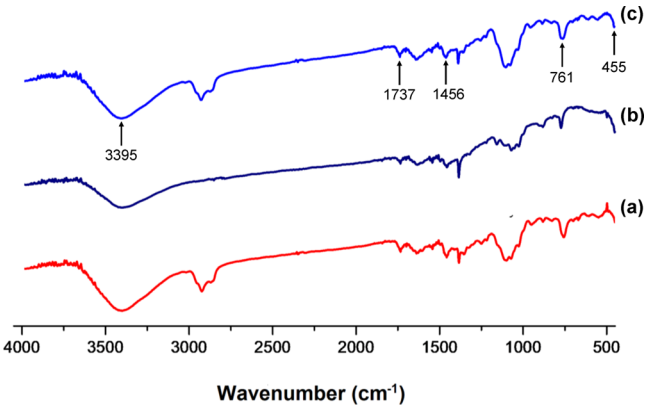

Figure 4. FTIR spectra of (a) LDH−[OH−C_6H_4COO], (b) CuNPs, and (c) CuNPs@LDH.

The model reaction was carried out under multiple sets of reactions to achieve the maximum conversion of cyclohexane. To improve the reaction conditions for the oxidation of cyclohexane, numerous variables such as oxidant effects, concentration of TBHP, concentration of catalysts, and reaction temperatures were fully investigated.

The influence of several oxidants (O_2, H_2O_2, and TBHP) was examined for the model reaction in determining the most effective oxidant. The reaction with O_2 and H_2O_2 gave low conversion of cyclohexane about 25.7 and 10.2%, whereas the selectivity of KA oil gave 74.9 and 81.2%, respectively. Surprisingly, when TBHP is employed instead of O_2 and H_2O_2 as an oxidant, a conversion of 31.4% is obtained and a selectivity of 87.3% with KA oil. All the sets of reactions were carried out at a temperature of 353 K, and the molar ratio of the oxidant to the substrate was 3:1 and the amount of the catalyst was kept constant at 25 mg. It is evident from the results that TBHP provides higher conversion and selectivity. Thus, TBHP was the appropriate oxidant selected for carrying out the desired reaction under solvent-free conditions.

Three different molar ratios of TBHP to cyclohexane (1, 2, and 3) were considered to examine the effect of the molar ratio of TBHP to cyclohexane at 353 K and used 75 mg of catalyst for 6 h, and the results listed in Table 3 and Figure 5a. Initially, when the molar ratio of cyclohexane to TBHP is 1, then conversion of cyclohexane (19.8%) with (80.7%) selectivity of KA oil was observed after a 6 h reaction time. Whereas the molar ratio of TBHP to cyclohexane is taken as 2, conversion was reached 33.5% with 93.1% selectivity of KA oil. Furthermore, on

https://doi.org/10.1021/acsomega.2c04425
ACS Omega 2022, 7, 41058−41068

Table 2. Catalytic Performance of Various Catalysts on the Oxidation of Cyclohexane[a]

		product selectivity (%)					
catalysts	conversion (%)	K	A	others[c]	KA oil	K/A (molar ratio)	TON
Blank	-	-	-	-	-	-	-
LDH	-	-	-	-	-	-	-
CuNPs	34.6	51.4	43.7	4.9	95.1	1.2	424
CuNPs@LDH	52.3	84.7	12.5	2.8	97.2	6.8	640
CuNPs@LDH[b]	-	-	-	-	-	-	-

[a]Reaction conditions: cyclohexane (20 mmol), TBHP (60 mmol), catalyst (75 mg), 353 K, 6 h; TON: turnover number. [b]2,6-Di-*tert*-butyl-4-methylphenol (BHT) as the free-radical scavenger is added in the reaction. [c]Cyclohexyl hydroperoxide, adipic acid, glutaric acid, succinic acid, hydroxyl hexylic acid, and ε-caprolactone.

Table 3. Influence of TBHP on Cyclohexane Oxidation over the CuNPs@LDH Nanocatalyst[a]

		product selectivity (%)					
TBHP:cyclohexane (molar ratio)	conversion (%)	K	A	others	KA oil	K/A (molar ratio)	TON
1	19.8	61.5	19.2	19.3	80.7	3.2	242
2	33.5	76.0	17.1	6.9	93.1	4.4	410
3	52.3	84.7	12.5	2.8	97.2	6.8	640

[a]Reaction conditions: cyclohexane (20 mmol), catalyst (75 mg), 353 K, 6 h; TON: turnover number.

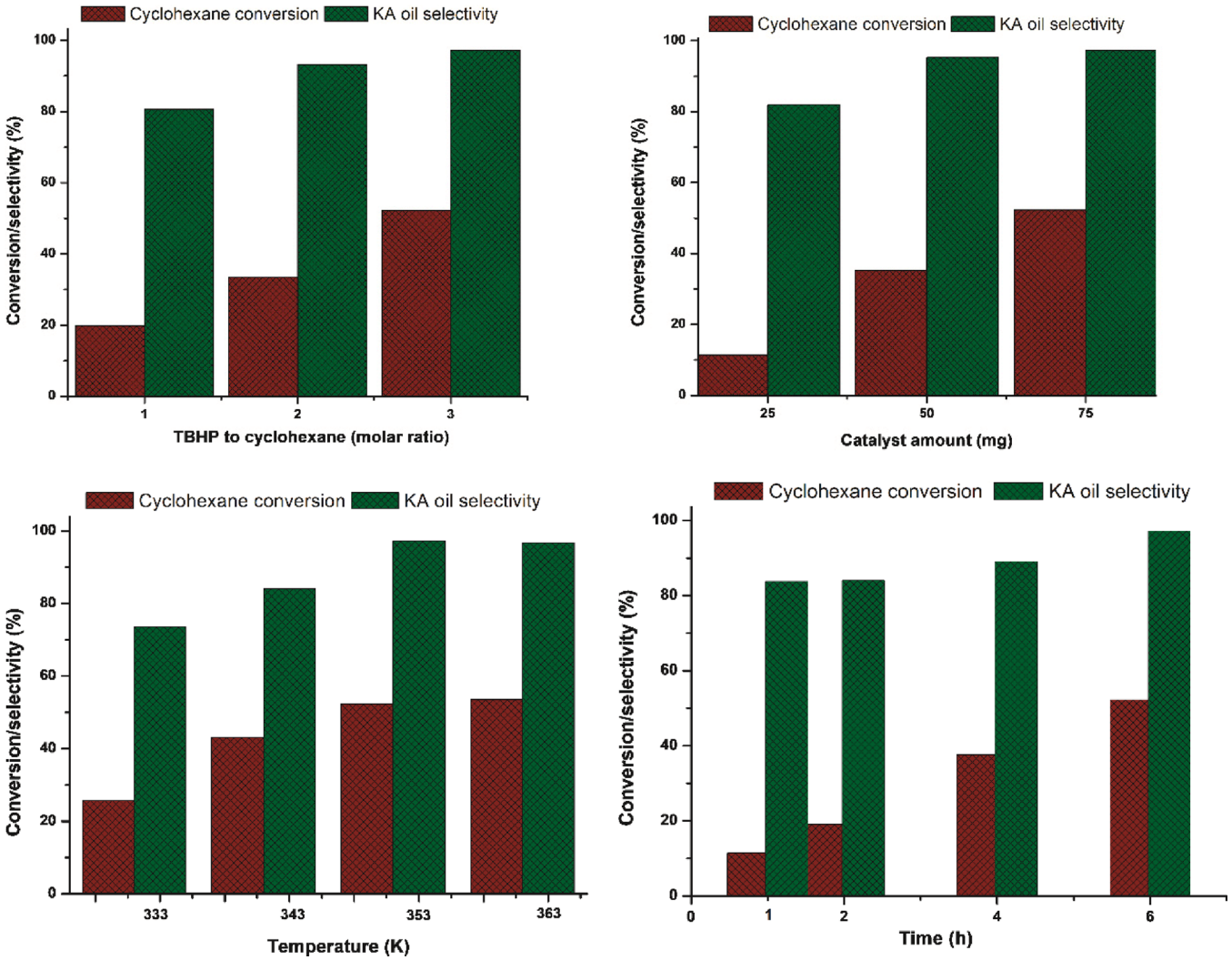

Figure 5. Optimization of reaction parameters and recycling. (a) Influence of TBHP molar ratio. (b) Influence of catalyst amount. (c) Influence of temperature. (d) Influence of time.

https://doi.org/10.1021/acsomega.2c04425
ACS Omega 2022, 7, 41058−41068

increasing the molar ratio of TBHP to cyclohexane to 3, conversion of cyclohexane increases to a maximum 52.3% with 97.2% selectivity of KA oil, whereas the selectivity of the other products was substantially lower.

Figure 5b depicts the impact of CuNPs@LDH nanocatalyst concentration on the oxidation of cyclohexane. While maintaining the other parameters constant, three different amounts of catalyst, specifically 25, 50, and 75 mg, were investigated. The results are given in Table 4. The initial result

Table 4. Influence of the Catalyst Amount on Oxidation of Cyclohexane over the CuNPs@LDH Nanocatalyst[a]

catalyst amount (mg)	conversion (%)	product selectivity (%)				K/A (molar ratio)	TON
		K	A	oth-ers	KA oil		
25	11.5	57.1	24.8	18.1	81.9	2.3	422
50	35.3	72.6	22.7	4.7	95.3	3.2	648
75	52.3	84.7	12.5	2.8	97.2	6.8	640

[a]Reaction conditions: cyclohexane (20 mmol), TBHP (60 mmol), 353 K, 6 h; TON: turnover number.

was observed when the concentration of the catalyst is 25 mg, where 11.5% conversion of cyclohexane was obtained with 81.9% KA oil selectivity. When the concentration of the catalyst is kept at 50 mg, then the conversion of cyclohexane achieves 35.3 and 95.3% selectivity of KA oil. Furthermore, when the catalyst amount is increased to 75 mg, the conversion of cyclohexane reaches a high of 52.3% with 97.2% selectivity of KA oil. It could be due to the high catalyst amount providing a large surface area. The catalyst amount increases from 25 to 50 mg and the TON increases from 422 to 648, while on further increasing the catalyst amount to 75 mg, the TON slightly decreases to 640. Based on the results presented above, 75 mg of catalyst is considered to be the optimal concentration of the catalyst.

The temperature has also influenced the oxidation of cyclohexane. To investigate the influence of temperature on cyclohexane oxidation, the temperature varied from 333, 343, and 353 K while the other parameters remained constant. It was noticed that when the temperature of the reaction was increased from 333 to 353 K, the conversion of cyclohexane improved from 25.8 to 52.3% and the selectivity of KA oil from 73.6 to 97.2%, respectively. Furthermore, increasing the temperature to 363 K marginally increases the conversion of cyclohexane (53.5%) while decreasing the selectivity of KA oil (94.7%) due to the decomposition of TBHP at higher temperature.[44] The results are depicted in Table 5 and Figure 5c. As the temperature rises from 333 to 353 K, the selectivity of KA oil and the TON steadily increases from 73.6 to 97.2% and 316 to 640, respectively. The investigation revealed that the highest conversion is obtained at 353 K; hence, this temperature is considered an optimum.

The influence of time over oxidation of cyclohexane is monitored at 1, 2, 4, and 6 h using a TBHP to cyclohexane molar ratio of 3 and a catalyst amount of 75 mg. Figure 5 and Table 6 illustrate that the conversion of cyclohexane increases linearly until 6 h and achieves 52.3% conversion of cyclohexane with 97.2% selectivity of KA oil.

Table 6. Influence of Time on Oxidation of Cyclohexane over the CuNPs@LDH Nanocatalyst[a]

time (h)	conversion (%)	product selectivity (%)				K/A (molar ratio)	TON
		K	A	oth-ers	KA oil		
0							
1	11.5	66.3	17.5	16.2	83.8	3.8	141
2	19.1	67.4	16.7	15.9	84.1	4.4	234
4	37.7	74.8	14.3	10.9	89.1	5.2	462
6	52.3	84.7	12.5	2.8	97.2	6.8	640

[a]Reaction conditions: cyclohexane (20 mmol), TBHP (60 mmol), catalyst (75 mg), temperature 353 K; TON: turnover number

2.3. Possible Reaction Pathway for Cyclohexane Oxidation. The initial step of oxidation is an initiation step, and the rate of initiation is highly dependent on coordination with metal centers.[45] In the presence of copper species (Cu^0/Cu^+), the oxidant TBHP may be decomposed into active radicals *t*-BuO• and *t*-BuOO• over the surface of the CuNPs@LDH nanocatalyst. Following this, *t*-BuO• radicals can extract H from cyclohexane to form cyclohexyl radicals. After this, the cyclohexane radicals would interact with *t*-BuOO•, which might originate from TBHP on the metal's surface, resulting in the formation of cyclohexyl-*t*-butyl hydroperoxide. Cyclohexyl-*t*-butyl hydroperoxide decomposes to cyclohexyl peroxy radicals and *t*-BuO• radicals, producing cyclohexanol and cyclohexanone.

A free-radical scavenger known as 2,6-di-*tert*-butyl-4-methylphenol (BHT) was introduced to this reaction as a quenching agent in order to confirm that the present reaction is a free-radical reaction over the CuNPs@LDH nanocatalyst. The experimental findings demonstrated that under optimized reaction conditions, no oxidation products were produced (Table 2). Because the addition of BHT, a radical scavenger, prevents the production of any products in the oxidation reaction, it is obvious that the oxidation of cyclohexane with *tert*-butyl hydroperoxide appears to be a radical process. As a consequence of the findings in this study and previous studies,[46,47] we proposed a probable reaction mechanism for the catalytic oxidation of cyclohexane with TBHP over CuNPs@LDH, as illustrated in Scheme 2.

Table 5. Influence of Temperature on Oxidation of Cyclohexane over the CuNPs@LDH Nanocatalyst[a]

temperature (K)	conversion (%)	product selectivity (%)				K/A (molar ratio)	TON
		K	A	others	KA oil		
333	25.8	51.7	21.9	26.4	73.6	2.3	316
343	43.1	67.4	16.7	15.9	84.1	4.4	528
353	52.3	84.7	12.5	2.8	97.2	6.8	640
363	53.5	80.4	14.3	5.3	94.7	5.6	655

[a]Reaction conditions: cyclohexane (20 mmol), TBHP (60 mmol), catalyst (75 mg), 6 h; TON: turnover number.

https://doi.org/10.1021/acsomega.2c04425
ACS Omega 2022, 7, 41058−41068

Scheme 2. Possible Reaction Pathway for the Cyclohexane Oxidation with TBHP over the CuNPs@LDH Nanocatalyst

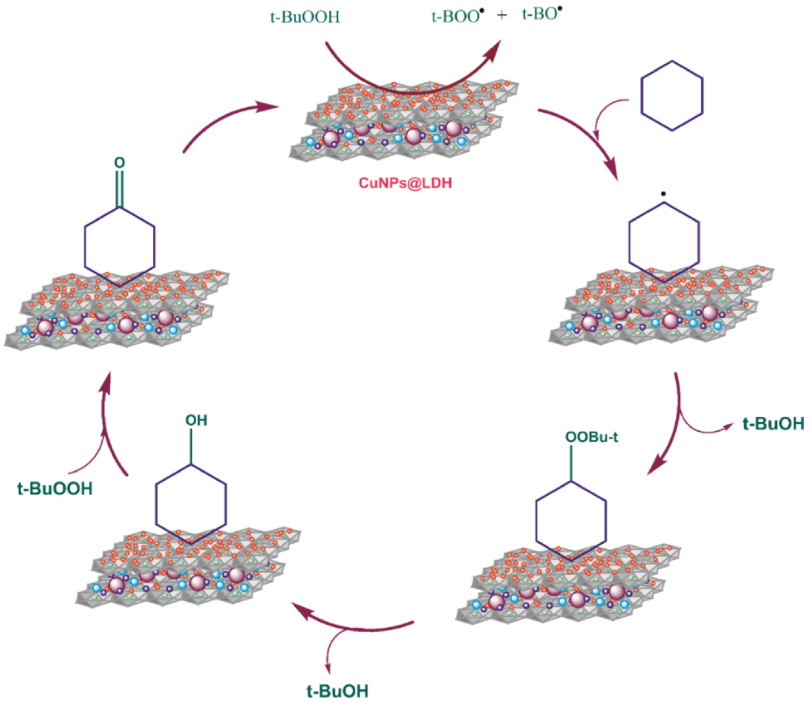

2.4. Hot Filter Experiment. The hot filter experiment was carried out to test the heterogeneity of the nanocatalyst. To minimize readsorption of leached copper onto the catalyst surface, the nanocatalyst was removed from the reaction mixture after 1 h of reaction in the first cycle. After 1 h of the first cycle, the filtrate was reintroduced into the reaction flask, and the reaction was continued for the following 5 h. After the reaction, the filtrates were collected to determine the amount of copper leached which was determined by ICP-AES. Copper was not found in significant amounts in the filtrates. Collected filtrates were also examined by gas chromatography and revealed that the rate of conversion did not increase further. The hot filter experiment results show that there was no metal leaching during the catalytic process. This finding suggests that the nanocatalyst was heterogeneous in nature.

2.5. Reusability of CuNPs@LDH Nanocatalysts. Catalyst recycling was tested and it was found that it can be reused up to six times in a row. The products were analyzed after each stage, and the heterogenized nanocatalyst was collected by filtering, properly washing, and reusing for a fresh set of cyclohexane oxidation studies. In a fresh process, no oxidation was identified in the filtrate. The recyclability of the CuNPs@LDH nanocatalyst is depicted in Figure 6. XRD, FTIR, EDX, and ICP-AES were used to further analyze the recovered nanocatalyst (Table 1). The copper content in the reused nanocatalyst was determined by ICP-AES analysis. Copper was not detected in substantial quantities in the filtrates. The decrease in catalytic activity might be attributed to the inevitable loss of the nanocatalyst throughout the collection process. On comparison of FTIR spectra and XRD patterns of the recycled nanocatalyst with the fresh nanocatalyst (Figure 7), it was observed that Cu nanoparticles supported on the LDH nanocatalyst do not exhibit any structural change after six successive cycles. This indicates that the nanocatalyst was stable during the catalytic process and may be recycled. The results demonstrate that there were no major alterations after recycling, suggesting that the CuNPs@LDH nanocatalyst was stable and reusable.

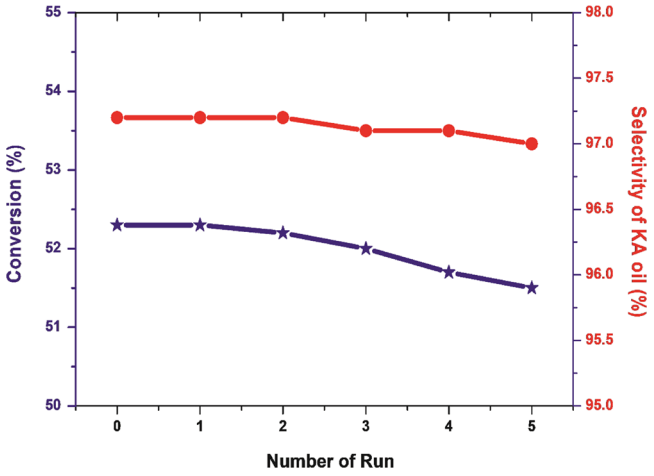

Figure 6. Recycling experiment of CuNPs@LDH.

3. CONCLUSIONS

In summary, we have reported a facile and promising method to synthesize CuNPs@LDH green nanocatalysts and evaluated their catalytic activity for the liquid phase oxidation of cyclohexane with TBHP used as a source of oxygen. The chemical reduction method was employed for the successful synthesis of CuNPs@LDH and achieved higher catalytic performance of about 52.3% conversion of cyclohexane with 97.2% selectivity of KA oil compared to pure Cu nanoparticles as well as many reported Cu-based catalysts. The hot filtration experiment proved that CuNPs@LDH was a heterogeneous catalyst and can be reused at least six times with almost the same activity. The current work proposes a new approach for developing a highly stable CuNPs@LDH nanocatalyst with potential applications in the oxidation of cyclohexane.

https://doi.org/10.1021/acsomega.2c04425
ACS Omega 2022, 7, 41058−41068

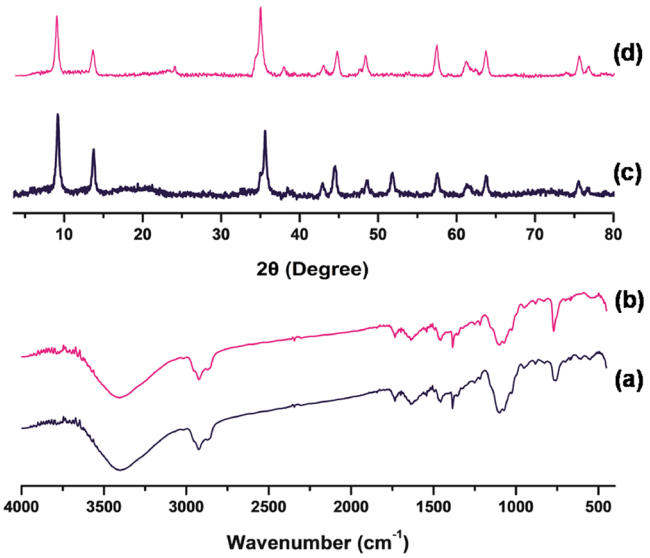

Figure 7. FTIR spectra of (a) fresh CuNPs@LDH and (b) reused CuNPs@LDH. XRD patterns of (c) fresh CuNPs@LDH and (d) reused CuNPs@LDH.

Furthermore, the oxidation of cyclohexane over CuNPs@LDH was preceded by a free-radical mechanism.

4. EXPERIMENTAL METHODS

4.1. Materials and Methods. All the materials were A.R. grade purchased from Merck and used without further purification. Powder XRD patterns of the samples were recorded on a Bruker D8 ADVANCE diffractometer in the 2θ range of 2−70° using CuKα radiation (λ = 1.5418 Å) at a scanning speed 2° per min with a step size of 0.02°. Scanning electron microscopy (SEM-EDAX) measurements were performed using a JEOL 6390LA/O XMX N electron microscope operating at 20 kV. Transmission electron microscopy (TEM-SEAD) studies were performed on a JEOL/JEM 2100 microscope. The FTIR spectra were recorded on a PerkinElmer model 1750 in KBr. Thermo Electron IRIS INTREPID II XSP DUO (ICP-AES) was used for the estimation of copper. The N_2 adsorption data, measured at 77 K by a volumetric adsorption setup (Micromeritics ASAP-2010, USA), were used to determine the BET surface area. Analytical gas chromatography was carried out on a Shimadzu gas chromatograph GC-14B with a dual-flame ionization detector (FID) and an attached Shimadzu printer having an Agilent SE-30 capillary column, 30 m × 0.32 mm. The products were identified by GC−MS (PerkinElmer Clarus 500 column; 30 m × 60 mm).

4.2. Synthesis of LDH−[OH−C_6H_4COO]. LDH−[OH−C_6H_4COO] was prepared by the coprecipitation method according to the previously reported procedure.[45] A solution of zinc acetate dihydrate (13.2 g) and aluminum(III) nitrate nonahydrate (7.5 g) was prepared in decarbonized water having a Zn−Al molar ratio of 3. To this mixture, a solution of salicylic acid (8.6 g) and NaOH (7.8 g) in decarbonized water was added with continuous stirring. Immediately a gel-like mixture was obtained, which was digested at 348 K for 50 h. Upon cooling, the product was isolated by filtration, washed with water followed by methanol, and the solid was dried at 333 K overnight.

4.3. Synthesis of Cu Nanoparticles. The synthesis of CuNPs was the chemical reduction according to the previously reported method with some modifications.[48] In a typical synthesis, 0.5 g of $CuSO_4.5H_2O$ was first dissolved in 50 mL of distilled water and then 5 mL of fructose solution (0.1 g) and 5 mL of NaOH solution (0.25 M) were added. The mixture was then kept at 353 K for 3 h. After cooling, the brown products were collected and washed several times with deionized water and ethanol in a row. The resulting product was dried at 353 K.

4.4. Synthesis of CuNPs@LDH. The CuNPs@LDH nanocatalyst was prepared by immobilization of CuNPs onto LDH−[OH−C_6H_4COO]. The LDH (1.0 g) was suspended in 50 mL of distilled water followed by an additional aqueous solution of copper(II) sulfate pentahydrate (0.35 g) under constant stirring at 353 K for 1 h. After stirring the mixture, fructose solution (0.1 g) and 10 mL of NaOH solution (0.25 M) were gradually added to the prepared solution with constant stirring and heating at 353 K for 5 h. The precipitates were separated from the solution by filtration and washed with deionized water and ethanol several times to take out the excessive fructose and dried at 373 K overnight.

4.5. General Route for the Catalytic Oxidation of Cyclohexane. The cyclohexane oxidation reaction proceeded in a 100 mL three-necked round-bottom flask equipped with a condenser. In a 25 mL three-necked round-bottom flask, a mixture of cyclohexane and TBHP in 1:3 molar ratio (in dodecane) and 75 mg of preactivated nanocatalyst was loaded. The mixture was then rapidly stirred for 5 h at 353 K using a magnetic stirrer with a hot plate. The reaction progress was monitored by taking aliquots from the reaction mixture at regular intervals and analyzing them with a gas chromatograph equipped with an FID detector. Gas chromatography was used to assess the conversion of cyclohexane and the selectivity of products produced after 5 h of reaction. The products were identified by using both known standards and GC−MS. After the reaction completion, the nanocatalyst was separated by filtering and washing multiple times with methanol and then acetone. It was then dried at 333 K for subsequent use.

The conversion (%), selectivity (%), and TON in the oxidation reaction is calculated as:[43,49]

$$\text{conversion (\%)} = \text{substrate converted (mmol)} / \text{substrate used (mmol)} \times 100$$

$$\text{selectivity (\%)} = \text{product formed (mmol)}] \text{ substrate used (mmol)} \times 100$$

$$\text{turn over number} = \text{mmol of products/mmol of catalysts}$$

AUTHOR INFORMATION

Corresponding Author

Jagat Singh Kirar − *Department of Chemistry, Government P.G. College, Guna, Madhya Pradesh 473001, India;* orcid.org/0000-0002-8022-5298; Email: j.skirar007@gmail.com

Authors

Neeraj Mohan Gupta − *Department of Chemistry, Government P.G. College, Guna, Madhya Pradesh 473001, India*

Kailash Chandra − *Department of Chemistry, Bareilly College, Bareilly, Uttar Pradesh 243005, India*

Hitesh Kumar Vani − *Department of Chemistry, Government College, Anjad, Madhya Pradesh 451556, India*

https://doi.org/10.1021/acsomega.2c04425
ACS Omega 2022, 7, 41058−41068

Savita Khare − *School of Chemical Sciences, Devi Ahilya University, Indore, Madhya Pradesh 452001, India;* orcid.org/0000-0002-2236-2948
Neha Tiwari − *School of Chemical Sciences, Devi Ahilya University, Indore, Madhya Pradesh 452001, India*
Yogesh Deswal − *Department of Chemistry, Guru Jambheshwar University of Science and Technology, Hisar, Haryana 125001, India*

Complete contact information is available at: https://pubs.acs.org/10.1021/acsomega.2c04425

Notes

The authors declare no competing financial interest.

■ ACKNOWLEDGMENTS

The authors are thankful to the Principal, Govt. P. G. College, Guna, and the Head of the Department for providing necessary facilities. We are also thankful to STIC, Cochin, for providing SEM, EDX, ICP, XRD, and HRTEM, and Material Analysis and Research Centre, Bengaluru, for providing the BET surface area facility.

■ REFERENCES

(1) Shilov, A.E.; Shulpin, G. B.*Activation and Catalytic Reactions of Saturated Hydrocarbons in the Presence of Metal Complexes*; Kluwer Academic Publishers: Dordrecht, 2000.
(2) Cavani, F.; Centi, G.; Perathoner, S.; Trifiro, F., Eds.; *Sustainable Industrial Processes*; Wiley-VCH: Weinheim, 2009.
(3) Zhang, J.; Liu, J.; Wang, X.; Mai, J.; Zhao, W.; Ding, Z.; Fang, Y. Construction of Z-scheme Tungsten Trioxide Nanosheets-Nitrogen-Doped Carbon Dots Composites for the Enhanced Photothermal Synergistic Catalytic Oxidation of Cyclohexane. *Appl. Catal., B* **2019**, *259*, No. 118063.
(4) Zhao, X.; Zhang, Y.; Wen, P.; Xu, G.; Ma, D.; Qiu, P. NH_2-MIL-125(Ti)/TiO_2 Composites as Superior Visible-Light Photocatalysts for Selective Oxidation of Cyclohexane. *Mol. Catal.* **2018**, *452*, 175−183.
(5) Schuchardt, U.; Cardoso, D.; Sercheli, R.; Pereira, R.; de Cruz, R. S.; Guerreiro, M. C.; Mandelli, D.; Spinace, E. V.; Fires, E. L. Cyclohexane oxidation continues to be a challenge. *Appl. Catal., A* **2001**, *211*, 1−17.
(6) Zou, G.; Zhong, W.; Xu, Q.; Xiao, J.; Liu, C.; Li, Y.; Mao, L.; Kirk, S.; Yin, D. Oxidation of Cyclohexane to Adipic Acid Catalyzed by Mn-Doped Titanosilicate with Hollow Structure. *Catal. Commun.* **2015**, *58*, 46−52.
(7) Wu, P.; Bai, P.; Loh, K. P.; Zhao, X. S. Au Nanoparticles Dispersed on Functionalized Mesoporous Silica for Selective Oxidation of Cyclohexane. *Catal. Today* **2010**, *158*, 220−227.
(8) Mizuno, N., Ed.; *Modern Heterogeneous Oxidation Catalysis: Design, Reactions and Characterization*; Wiley-VCH: Weinheim, 2009.
(9) Clerici, M. G.; Kholdeeva, O. A., Eds.; *Liquid Phase Oxidation via Heterogeneous Catalysis: Organic Synthesis and Industrial Applications*; Wiley: Hoboken, New Jersey, 2013.
(10) Han, X.; Liu, Y.; Qi, Z.; Zhang, Q.; Zhao, P.; Wang, L.; Gao, L.; Zheng, G. Graphene supported CoO nanoparticles as an advanced catalyst for aerobic oxidation of cyclohexane. *New J. Chem.* **2022**, *46*, 2792−2797.
(11) Liu, P.; You, K.; Deng, R.; Chen, Z.; Jian, J.; Zhao, F.; Liu, P.; Ai, Q.; Luo, H. Hydrotalcite-derived Co-MgAlO mixed metal oxides as efficient and stable catalyst for the solvent-free selective oxidation of cyclohexane with molecular oxygen. *Mol. Catal.* **2019**, *466*, 130−137.
(12) Jian, J.; Yang, D.; Liu, P.; You, K.; Sun, W.; Zhou, H.; Yuan, Z.; Ai, Q.; Luo, H. Solvent-Free Partial Oxidation of Cyclohexane to KA Oil over Hydrotalcite-Derived Cu-MgAlO Mixed Metal Oxides. *Chin. J. Chem. Eng.* **2022**, *42*, 269−276.
(13) Ziouèche, A.; Cherif-Aouali, L.; Bengueddach, A. Liquid phase oxidation of cyclohexane over mesoporous cobalt silicates molecular sieves synthesized in strong acidic media by assembly of preformed CoS-1 precursors with triblock copolymer. *J. Porous Mater.* **2019**, *26*, 575−581.
(14) Huang, G.; Liu, Y.; Cai, J. L.; Chen, X. F.; Zhao, S. K.; Guo, Y. A.; Wei, S. J.; Li, X. Heterogeneous biomimetic catalysis using iron porphyrin for cyclohexane oxidation promoted by chitosan. *Appl. Surf. Sci.* **2017**, *402*, 436−443.
(15) Shahzeydi, A.; Ghiaci, M.; Farrokhpour, H.; Shahvar, A.; Sun, M.; Saraji, M. Facile and Green Synthesis of Copper Nanoparticles Loaded on the Amorphous Carbon Nitride for the Oxidation of Cyclohexane. *Chem. Eng. J.* **2019**, *370*, 1310−1321.
(16) Machado, K.; Mukhopadhyay, S.; Mishra, G. S. Nanoparticles Silica Anchored Cu(II) and V(IV) Scorpionate Complexes for Selective Catalysis of Cyclohexane Oxidation. *J. Mol. Catal. A: Chem.* **2015**, *400*, 139−146.
(17) Xiao, Y.; Liu, J.; Mai, J.; Pan, C.; Cai, X.; Fang, Y. High-Performance Silver Nanoparticles Coupled with Monolayer Hydrated Tungsten Oxide Nanosheets: The Structural Effects in Photocatalytic Oxidation of Cyclohexane. *J. Colloid Interface Sci.* **2018**, *516*, 172−181.
(18) Liu, L.; Arenal, R.; Meira, D. M.; Corma, A. Generation of Gold Nanoclusters Encapsulated in an MCM-22 Zeolite for the Aerobic Oxidation of Cyclohexane. *Chem. Commun.* **2019**, *55*, 1607−1610.
(19) Sun, L.; Liu, J.; Luo, W.; Yang, Y.; Wang, F.; Weerakkody, C.; Suib, S. L. Preparation of Amorphous Copper - Chromium Oxides Catalysts for Selective Oxidation of Cyclohexane. *Mol. Catal.* **2018**, *460*, 16−26.
(20) Gawande, M. B.; Goswami, A.; Felpin, F. X.; Asefa, T.; Huang, X.; Silva, R.; Zou, X.; Zboril, R.; Varma, R. S. Cu and Cu-Based Nanoparticles: Synthesis and Applications in Catalysis. *Chem. Rev.* **2016**, *116*, 3722−3811.
(21) Wu, P.; Xiong, Z.; Loh, K. P.; Zhao, X. S. Selective Oxidation of Cyclohexane over Gold Nanoparticles Supported on Mesoporous Silica Prepared in the Presence of Thioether Functionality. *Catal. Sci. Technol.* **2011**, *1*, 285−294.
(22) Zhang, H.; Guo, W.; Lu, N.; Fan, B. Solvent-Free Selective Oxidation of Aromatic Alcohol with O_2 over MgAl-LDH Supported Pd Nanoparticles: Effects of Preparation Methods and Solvents. *Mater. Chem. Phys.* **2020**, *252*, No. 123193.
(23) Miao, M. Y.; Feng, J. T.; Jin, Q.; He, Y. F.; Liu, Y. N.; Du, Y. Y.; Zhang, N.; Li, D. Q. Hybrid Ni−Al layered double hydroxide/graphene composite supported gold nanoparticles for aerobic selective oxidation of benzyl alcohol. *RSC Adv.* **2015**, *5*, 36066−36074.
(24) Choudhary, A.; Sharma, N.; Sharma, C.; Jamwal, B.; Paul, S. Synergistic Effect of Cr^{3+} on Layered Double Hydroxide Supported Cu^0 Nanoparticles for the Oxidation of Alcohols and Hydrocarbons. *ChemistrySelect* **2019**, *4*, 5276−5283.
(25) Daud, M.; Hai, A.; Banat, F.; Wazir, M. B.; Habib, M.; Bharath, G.; Al-Harthi, M. A. Review on the Recent Advances, Challenges and Future Aspect of Layered Double Hydroxides (LDH)−Containing Hybrids as Promising Adsorbents for Dyes Removal. *J. Mol. Liq.* **2019**, *288*, No. 110989.
(26) Lu, L.; Li, J.; Ng, D. H. L.; Yang, P.; Song, P.; Zuo, M. Synthesis of Novel Hierarchically Porous Fe_3O_4@MgAl−LDH Magnetic Microspheres and Its Superb Adsorption Properties of Dye from Water. *J. Ind. Eng. Chem.* **2017**, *46*, 315−323.
(27) Takemoto, M.; Tokudome, Y.; Murata, H.; Okada, K.; Takahashi, M.; Nakahira, A. Synthesis of High-Specific-Surface-Area Li-Al Mixed Metal Oxide: Through Nanoseed-Assisted Growth of Layered Double Hydroxide. *Appl. Clay Sci.* **2021**, *203*, No. 106006.
(28) Mahpudz, A.; Lim, S. L.; Inokawa, H.; Kusakabe, K.; Tomoshige, R. Cobalt Nanoparticle Supported on Layered Double Hydroxide: Effect of Nanoparticle Size on Catalytic Hydrogen Production by $NaBH_4$ Hydrolysis. *Environ. Pollut.* **2021**, *290*, No. 117990.
(29) Kirar, J. S.; Khare, S.; Tiwari, N. Cu(II) and Co(II) Schiff-Base Complexes Immobilized on Layered Double Hydroxide: Synthesis, Characterizations, DFT Calculations and Catalytic Activity. *ChemistrySelect* **2021**, *6*, 11557−11568.
(30) Kirar, J. S.; Khare, S.; Tiwari, N. Transition Metal Schiff Base Complexes Supported on Layered Double Hydroxide: Synthesis,

Characterization and Catalytic Activity for the Oxidation of Toluene. *React. Kinet., Mech. Catal.* **2021**, *132*, 1025−1046.
(31) Abderrazek, K.; Srasra, N. F.; Srasra, E. Synthesis and Characterization of [Zn-Al] Layered Double Hydroxides: Effect of the Operating Parameters. *J. Chin. Chem. Soc.* **2017**, *64*, 346−353.
(32) Sertsova, A. A.; Subcheva, E. N.; Yurtov, E. V. Synthesis and Study of Structure Formation of Layered Double Hydroxides Based on Mg, Zn, Cu, and Al. *Russ. J. Inorg. Chem.* **2015**, *60*, 23−32.
(33) Ahmed, A. A. A.; Talib, Z. A.; Hussein, M. Z.; Zakaria, A. Zn−Al layered double hydroxide prepared at different molar ratios: Preparation, characterization, optical and dielectric properties. *J. Solid State Chem.* **2012**, *191*, 271−278.
(34) Rathee, G.; Kohli, S.; Panchal, S.; Singh, N.; Awasthi, A.; Singh, S.; Singh, A.; Hooda, S.; Chandra, R. Fabrication of a Gold-Supported NiAlTi-Layered Double Hydroxide Nanocatalyst for Organic Transformations. *ACS Omega* **2020**, *5*, 23967−23974.
(35) Feng, L.; Zhang, C.; Gao, G.; Cui, D. Facile Synthesis of Hollow Cu_2O Octahedral and Spherical Nanocrystals and Their Morphology-Dependent Photocatalytic Properties. *Nanoscale Res. Lett.* **2012**, *7*, 276.
(36) Aslam, M.; Gopakumar, G.; Shoba, T. L.; Mulla, I. S.; Vijayamohanan, K.; Kulkarni, S. K.; Urban, J.; Vogel, W. Formation of Cu and Cu_2O Nanoparticles by Variation of the Surface Ligand: Preparation, Structure, and Insulating-to-Metallic Transition. *J. Colloid Interface Sci.* **2002**, *255*, 79−90.
(37) Damodara, D.; Arundhathi, R.; Likhar, P. R. Copper Nanoparticles from Copper Aluminum Hydrotalcite: An Efficient Catalyst for Acceptor- and Oxidant-Free Dehydrogenation of Amines and Alcohols. *Adv. Synth. Catal.* **2014**, *356*, 189−198.
(38) Dong, X.; Wang, Z.; Yuan, Y.; Yang, Y. Synergistic Catalysis of Cu^+/Cu^0 for Efficient and Selective N-Methylation of Nitroarenes with Para-Formaldehyde. *J. Catal.* **2019**, *375*, 304−313.
(39) Nityashree, N.; Menezes, P. Mg/Al layered double hydroxide-Pt nanoparticle composite by delamination-restacking route. *Appl. Nanosci.* **2013**, *3*, 321−327.
(40) Liu, Y.; Zhou, R.; Qu, J.; Han, F.; Zhang, S.; Xu, X. Cu Nanoparticles-Dispersed Mg-Al Layered Double Hydroxides as Efficient Catalysts for CO_2 Conversion with Propargyl Alcohols. *Appl. Catal., A* **2022**, *630*, No. 118444.
(41) Kirar, J. S.; Khare, S. Selective Oxidation of Ethylbenzene to Acetophenone over Cr(III) Schiff Base Complex Intercalated into Layered Double Hydroxide. *Appl. Organomet. Chem.* **2018**, *32*, No. e4408.
(42) Khare, S.; Singh Kirar, J.; Parashar, S. Solvent-Free Oxidation of Ethylbenzene over LDH-Hosted Co(II) Schiff Base of 2-Hydroxy-1-Naphthaldehyde and 4-Amino Benzoic Acid. *Inorg. Nano-Metal Chem.* **2019**, *49*, 204−216.
(43) Xiao, Y.; Liu, J.; Xie, K.; Wang, W.; Fang, Y. Aerobic oxidation of cyclohexane catalyzed by graphene oxide: Effects of surface structure and functionalization. *Mol. Catal.* **2017**, *431*, 1−8.
(44) Khare, S.; Chokhare, R.; Shrivastava, P.; Kirar, J. S.; Parashar, S. α-Zirconium phosphate supported metal−salen complex: synthesis, characterization and catalytic activity for cyclohexane oxidation. *J. Porous Mater.* **2017**, *24*, 855−866.
(45) Kirar, J. S.; Khare, S. Cu(II) Schiff Base Complex Intercalated into Layered Double Hydroxide for Selective Oxidation of Ethylbenzene under Solvent-Free Condition. *RSC Adv.* **2018**, *8*, 18814.
(46) Xie, C.; Wang, W.; Yang, Y.; Jiang, L.; Chen, Y.; He, J.; Wang, J. Enhanced Stability and Activity for Solvent-Free Selective Oxidation of Cyclohexane over Cu_2O/CuO Fabricated by Facile Alkali Etching Method. *Mol. Catal.* **2020**, *495*, No. 111134.
(47) Zaccheria, F.; Ravasio, N.; Psaro, R.; Fusi, A. Synthetic Scope of Alcohol Transfer Dehydrogenation Catalyzed by Cu/Al_2O_3: A New Metallic Catalyst with Unusual Selectivity. *Chem. − Eur. J.* **2006**, *12*, 6426−6431.
(48) Khan, A.; Rashid, A.; Younas, R.; Chong, R. A Chemical Reduction Approach to the Synthesis of Copper Nanoparticles. *Int. Nano Lett.* **2016**, *6*, 21−26.
(49) Tordin, E.; List, M.; Monkowius, U.; Schindler, S.; Knör, G. Synthesis and characterisation of cobalt, nickel and copper complexes with tripodal 4N ligands as novel catalysts for the homogeneous partial oxidation of alkanes. *Inorg. Chim. Acta* **2013**, *402*, 90−96.

https://doi.org/10.1021/acsomega.2c04425
ACS Omega 2022, 7, 41058−41068